

# A high precision U–Pb radioisotopic age for the Agrio Formation, Neuquén Basin, Argentina: Implications for the chronology of the Hauterivian Stage



Beatriz Aguirre-Urreta <sup>a,\*</sup>, Mark Schmitz <sup>b</sup>, Marina Lescano <sup>a</sup>, Maisa Tunik <sup>c</sup>, Peter F. Rawson <sup>d,e</sup>, Andrea Concheyro <sup>a</sup>, Mariano Buhler <sup>f</sup>, Víctor A. Ramos <sup>a</sup>

<sup>a</sup> Instituto de Estudios Andinos Don Pablo Groeber (UBA-CONICET), Universidad de Buenos Aires, Ciudad Universitaria, Pabellón 2, 1428, Buenos Aires, Argentina

<sup>b</sup> Department of Geosciences, Boise State University, 1910 University Drive Boise, Idaho, ID, 83725, USA

<sup>c</sup> Universidad de Río Negro, Sede Alto Valle, 8332, General Roca, Río Negro, Argentina

<sup>d</sup> School of Environmental Sciences, University of Hull, Cottingham Road, Hull, HU6 7RX, UK

<sup>e</sup> Department of Earth Sciences, University College London, Gower Street, London, WC1E 6BT, UK

<sup>f</sup> YPF S.A., Talero 360, 8300, Neuquén, Argentina

## ARTICLE INFO

### Article history:

Received 16 November 2016

Accepted in revised form 26 March 2017

Available online 30 March 2017

### Keywords:

Geochronology

Biostratigraphy

Ammonites

Nannofossils

Cretaceous

## ABSTRACT

A new CA-ID TIMS U–Pb age of  $130.39 \pm 0.16$  Ma is presented here from the Pilmatué Member of the Agrio Formation, lower Hauterivian of the Neuquén Basin in west-central Argentina. This high precision radioisotopic new age, together with the two former ones from the upper Hauterivian Agua de la Mula Member of the Agrio Formation and modern cyclostratigraphic studies in the classical sections of the Mediterranean Province of the Tethys indicate that the Hauterivian Stage spans some 6 Ma, starting *ca.* 132 Ma and ending *ca.* 126 Ma. These radioisotopic ages are tied to ammonite biostratigraphy and calcareous nannofossil bioevents and biozones recognized in the Neuquén Basin which in turn are correlated with the Mediterranean standard zones. A new geological time scale for the Valanginian–Hauterivian stages in the Mediterranean region integrating astrochronological and radiochronological data differs with the current official geological time scale which still maintains poorly constraint absolute ages for the Berriasian–Aptian interval.

© 2017 Elsevier Ltd. All rights reserved.

## 1. Introduction

Up to now, the global ‘standard’ Upper Jurassic and Lower Cretaceous stages have been based on stratigraphic sections in the Mediterranean Province of the Tethys, and are mostly defined by ammonite biostratigraphy and calcareous nannofossil bioevents that have been calibrated with the M sequence of geomagnetic polarity chronos. But the lack of precise radioisotopic ages from this region has hindered the construction of an accurate Late Jurassic and Early Cretaceous numerical time scale despite the efforts of the International Commission on Stratigraphy (Cohen et al., 2013). Since the international stratigraphic chart published by Remane

(2000), each four years a new global geological time scale has been produced (Gradstein et al., 2004, 2012, Ogg et al., 2008, 2016). But only slight adjustments are proposed in these successive contributions to the Late Jurassic and Early Cretaceous timescale and the boundaries between stages and their duration remain uncertain (including the important Jurassic/Cretaceous boundary).

Our studies in the Neuquén Basin in west-central Argentina are aimed at reducing these uncertainties. Here numerous tuff bands occur, interbedded with often richly-fossiliferous sediments. Vennari et al. (2014) and Aguirre-Urreta et al. (2015) provided high precision radioisotopic ages which are beginning to fill a gap of over 14 million years in the numerical calibration of the current global Early Cretaceous geological time scale.

A new CA-ID TIMS U–Pb age of  $130.39 \pm 0.16$  Ma is presented here from the Pilmatué Member of the Agrio Formation. The measured section is El Portón (Fig. 1A) where a tuff layer is interbedded with beds containing ammonites indicating the base of the

\* Corresponding author. Instituto de Estudios Andinos Don Pablo Groeber (UBA-CONICET), Universidad de Buenos Aires, Ciudad Universitaria, Pabellón 2, 1428, Buenos Aires, Argentina.

E-mail address: [aguirre@gl.fcen.uba.ar](mailto:aguirre@gl.fcen.uba.ar) (B. Aguirre-Urreta).

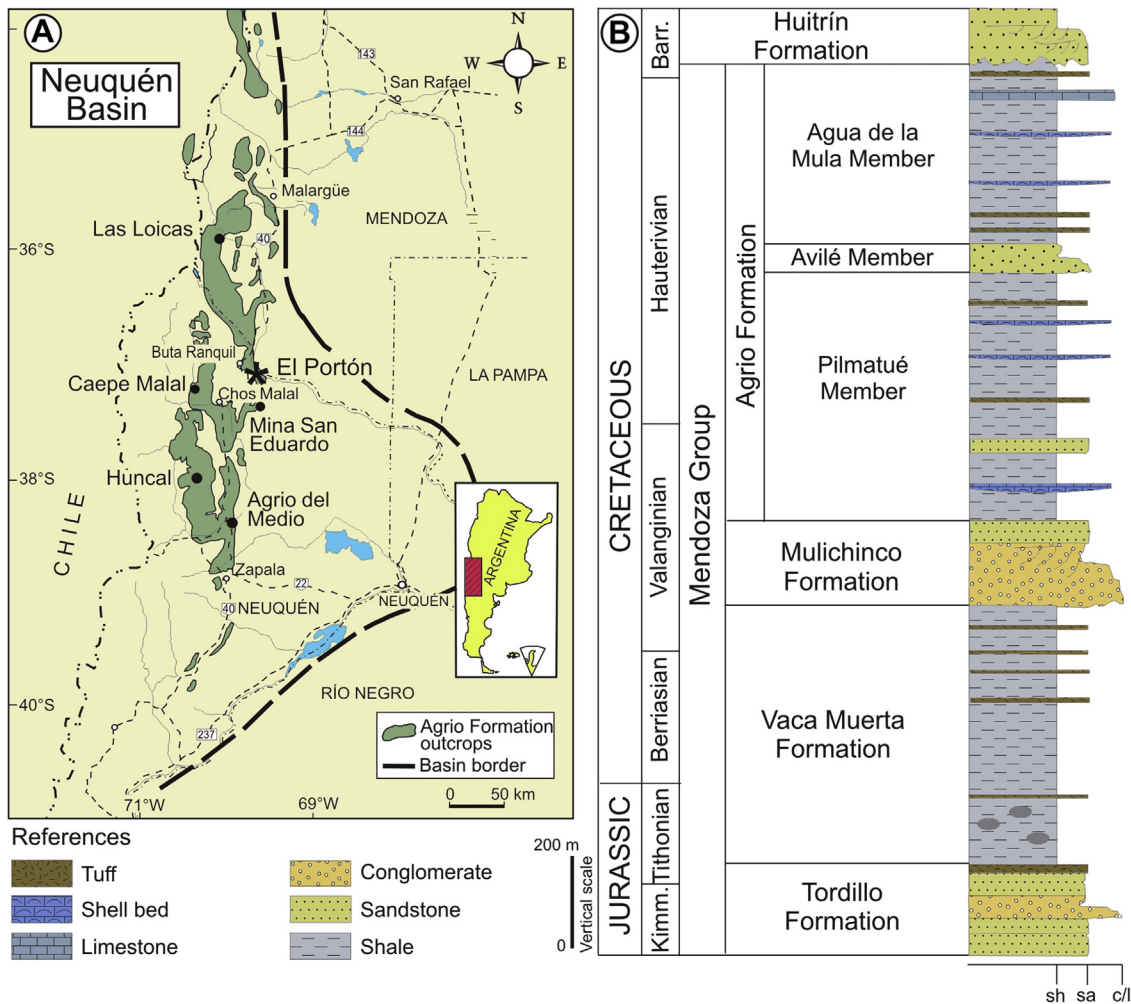


**Fig. 1.** A. The Neuquén Basin in west-central Argentina with exposures of the Agrio Formation and localities cited in the text. B. Generalized stratigraphic column of the Mendoza Group.

*Holcoptychites agrioensis* subzone, *Holcoptychites neuquensis* zone, of the early Hauterivian. The Neuquén Basin (Austral) ammonite sequence can be correlated with that of the Mediterranean Province of the Tethyan Realm (Reboulet et al., 2014) while two calcareous nannofossils bioevents recognized in the section also provide tie points with the same events recognized in the Northern Hemisphere.

This new age, together with the two former ones provided by Aguirre-Urreta et al. (2015) from the Neuquén Basin and the cyclostratigraphic studies by Martínez et al. (2015) in the classical sections of the Mediterranean Province of the Tethys indicate that the Hauterivian Stage spans some 6 Myr, starting ca. 132 Ma and ending ca. 126 Ma.

## 2. The Neuquén Basin

### 2.1. Geological setting

The Neuquén Basin is a triangular-shaped, retroarc basin, covering more than 160,000 km<sup>2</sup> that developed in a normal subduction segment at the foothills of the Andes in west-central Argentina (Legarreta and Uliana, 1991; Ramos, 2010) (Fig. 1A). The complex history of the basin began with Triassic rift deposits during a phase of continental extension. Afterwards, the basin was subject to thermal subsidence and eustatic sea level changes. Marine

transgressions from the Pacific Ocean led to the deposition of a Jurassic-Cretaceous sedimentary succession more than 7 km thick with several petroleum source rock units and reservoir intervals (Vergani et al., 1995). In the Late Cretaceous a change in tectonic setting led to inversion of the basin and the formation of a fold-and-thrust belt (Ramos, 2010). The last marine deposits in the area (Upper Cretaceous-Paleocene) are related to a transgression from the Atlantic Ocean. Sedimentation then continued under continental conditions, producing synorogenic Tertiary strata which in turn are covered by widespread volcanic rocks of Tertiary or Quaternary ages (Ramos and Folguera, 2005).

The infill of the Neuquén Basin during the Late Jurassic-Early Cretaceous is represented by both marine and continental deposits that are placed in the Mendoza Group (from base to top, Tordillo, Vaca Muerta, Mulichinco/Chachao and Agrio Formations) (Groebner, 1953; Legarreta and Uliana, 1991) (Fig. 1B). Laterally continuous outcrops and an abundant fossil record, combined with the interbedded tuffs, make the basin an excellent site to carry out integrated stratigraphical, paleontological, and radioisotopic studies.

### 2.2. The Agrio Formation

A transgressive phase in the late early Valanginian led to the deposition of the shales, limestones and sandstones of the Agrio Formation. This unit rests on the Mulichinco Formation of

continental to coastal sandstones and shales in the northern and southern part of the basin, and on its time equivalent sequence, the shelf carbonates of the Chachao Formation, in the central area (Legarreta and Uliana, 1991). The Agrio Formation is covered by the sandstones, evaporites and limestones of the Huitrín Formation, indicating the regression of the Pacific sea that commenced in Barremian times (Aguirre-Urreta et al., 2008; Lazo and Damborenea, 2011).

Weaver (1931) divided the Agrio Formation into lower and upper members separated by a thin but laterally persistent sandstone, the Avilé Member. Both the lower or Pilmatué Member and the upper or Agua de la Mula Member (Leanza and Hugo, 2001) are marine and mainly composed of massive clay shales interbedded with thin layers of packstones, wackestones, rudstones and floatstones. The intervening Avilé Sandstone Member consists of some 25–40 m of yellowish brown coarse sandstones, often cross-bedded. It is non-marine and marks a significant sea-level fall across the basin (Gulisano and Gutiérrez Pleimling, 1988; Veiga et al., 2002). The sandstone provides an excellent marker horizon, generally forming a distinct topographic feature.

The complete Agrio Formation, 620 m thick, was measured at the locality El Portón ( $37^{\circ}11'S$ ;  $69^{\circ}40'W$ ) on the eastern flank of the Pampa Tril anticline (Fig. 2). This locality is 6.5 km south from El Portón oil field and some 22 km southeast of Buta Ranquil along a local dirt road. Only the Pilmatué Member is described below, 300 m thick, which was measured along a dry creek (Fig. 3).

The first 110 m are mostly composed of dark calcareous shales, thinly laminated, interbedded with sparse thin limestones. Two intervals, one at the base and other between 35 and 45 m, contain numerous calcareous nodules and large foraminifera (*Epistomina* sp.). A few, thin tuffs are also present. Between 110 and 143 m, the number of limestones and tuffs increases, and the shales become less conspicuous and lighter in color. A new interval of very dark, laminated shales interbedded with thin limestones is represented between 143 and 160 m. Two distinctive horizons contain galleries of *Thalassinoides* isp. (Fig. 3). Up section to 240 m, the succession is composed of dark calcareous shales interbedded with numerous limestones and tuffs. The common limestone types along the section are massive mudstones, but bioclastic mudstones are also recognized (Fig. 3). The final 60 m of the section up to the Avilé Member are composed of very dark laminated shales, sparse limestones, and an interval with calcareous nodules and numerous thin tuffs. Besides the ammonites, two distinctive horizons with Inoceramid bivalves were identified.

The tuff analyzed here, POT 3, is located 180 m above the base of the section. It is a light yellowish, massive, coarse grained tuff. In thin section altered feldspar grains and cuspatate pumice shards replaced by calcite were observed in an altered matrix (Fig. 4A–B).

### 3. Material and methods

#### 3.1. U–Pb zircon geochronology

Ash samples were collected from cleaned bedding planes to avoid contamination with soil and surrounding sedimentary rocks. In the laboratory, samples were prepared by conventional density and magnetic methods. Single grain U–Pb dating was conducted in the Boise State University Isotope Geology Laboratory.

The entire zircon separate was placed in a muffle furnace at 900 °C for 60 h in quartz beakers to anneal minor radiation damage; annealing enhances cathodoluminescence (CL) emission (Nasdala et al., 2002), promotes more reproducible interelement fractionation during laser ablation inductively coupled plasma mass spectrometry (LA-ICPMS) (Allen and Campbell, 2012), and prepares the crystals for subsequent chemical abrasion (Mattinson, 2005). Following annealing, individual grains were hand-picked and mounted, polished and imaged by cathodoluminescence (CL) on a scanning electron microscope. From these compiled images, grains with consistent and dominant CL patterns were selected for further isotopic analysis.

U–Pb geochronology methods for isotope dilution thermal ionization mass spectrometry follow those previously published by Davydov et al. (2010) and Schmitz and Davydov (2012). Zircon crystals were subjected to a modified version of the chemical abrasion method of Mattinson (2005), whereby single crystal fragments plucked from grain mounts were individually abraded in a single step with concentrated HF at 190 °C for 12 h. All analyses were undertaken on crystals previously mounted, polished and imaged by cathodoluminescence (CL), and selected on the basis of zoning patterns. U–Pb dates and uncertainties for each analysis were calculated using the algorithms of Schmitz and Schoene (2007) and the U decay constants of Jaffey et al. (1971). Uncertainties are based upon non-systematic analytical errors, including counting statistics, instrumental fractionation, tracer subtraction, and blank subtraction. These error estimates should be considered when comparing our  $^{206}\text{Pb}/^{238}\text{U}$  dates with those from other laboratories that used tracer solutions calibrated against the EARTHTIME gravimetric standards. When comparing our dates with those derived from other decay schemes (e.g.,  $^{40}\text{Ar}/^{39}\text{Ar}$ ,  $^{187}\text{Re}-^{187}\text{Os}$ ), the uncertainties in tracer calibration (0.03%; Condon et al., 2015; McLean et al., 2015) and U decay constants (0.108%; Jaffey et al., 1971) should be added to the internal error in quadrature. Quoted errors for calculated weighted means are thus of the form  $\pm X(Y)[Z]$ , where X is solely analytical uncertainty, Y is the combined analytical and tracer uncertainty, and Z is the combined analytical, tracer and  $^{238}\text{U}$  decay constant uncertainty.



**Fig. 2.** Panoramic view, looking east, of the Pilmatué Member of the Agrio Formation at El Portón.

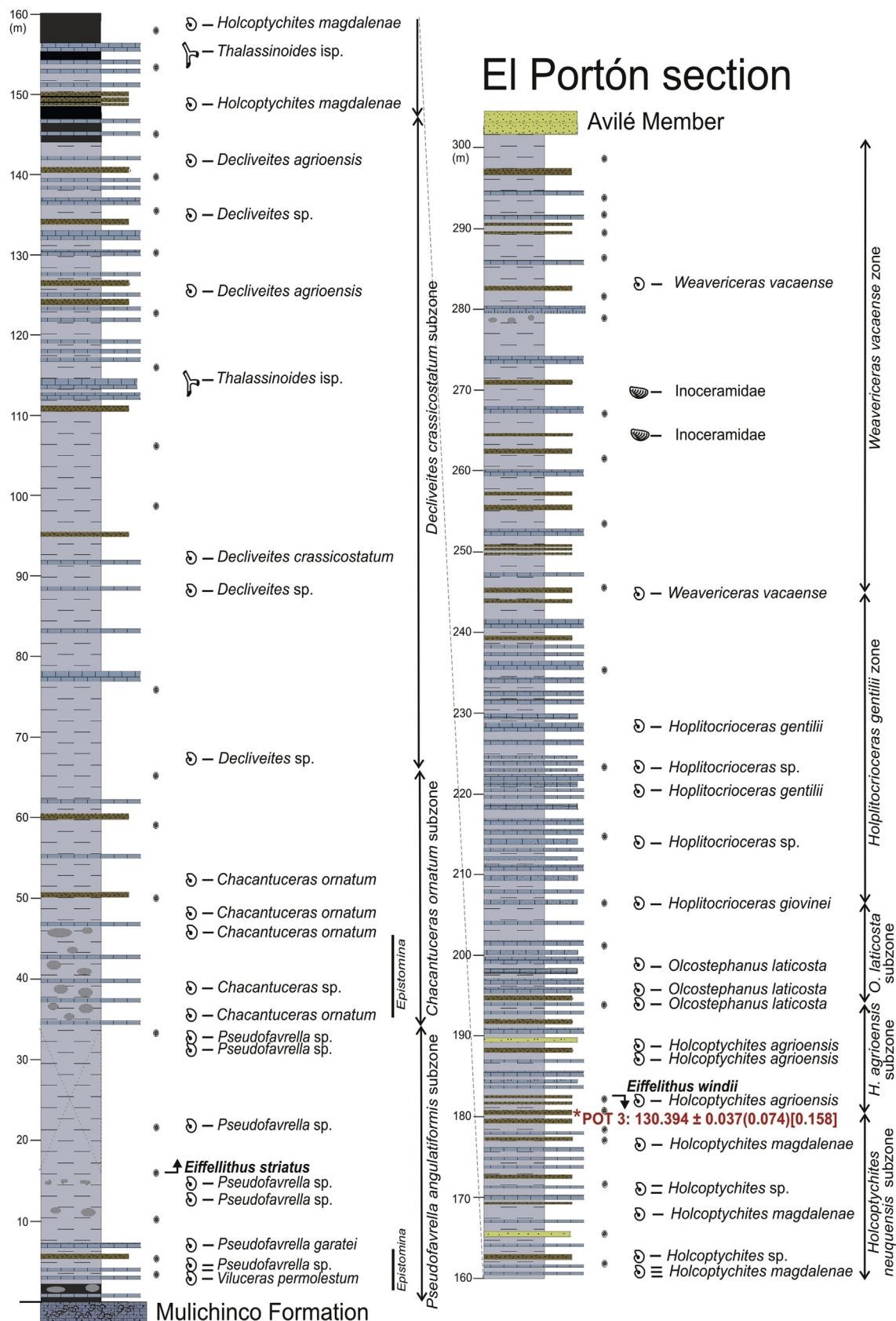


**Fig. 3.** The Pilmatué Member of the Agrio Formation at El Portón, with indication of nannofossil samples and ammonite levels.

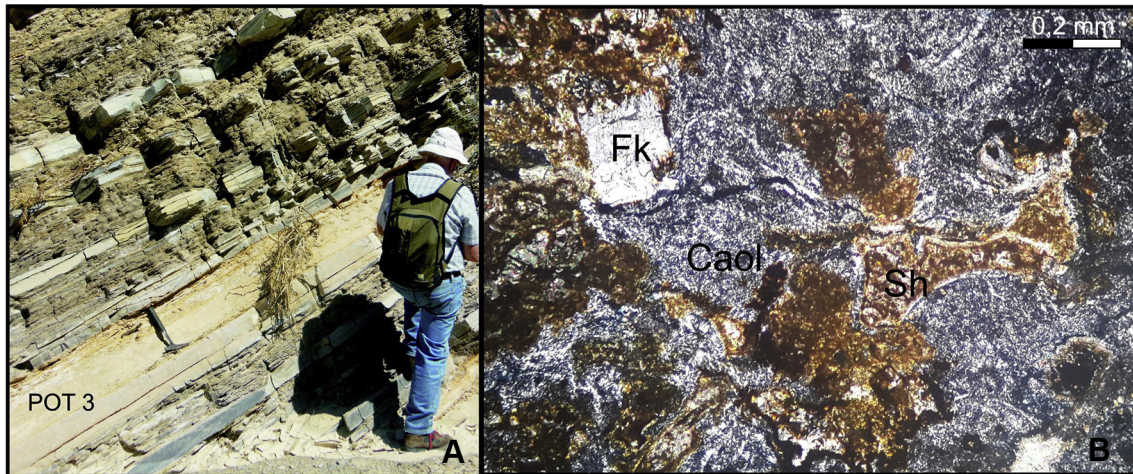


**Fig. 4.** A. The 35 cm thick POT 3 tuff interbedded with dark shales and limestones at the base of the *Holcoptychites agrioensis* ammonite subzone. B. Thin section of POT 3 tuff showing altered feldspar grains and cuspatate and pumice shards replaced by calcite.

### 3.2. Ammonites

Ammonite specimens in this study were registered from 43 levels in the Pilmatué Member of the Agrio Formation at El Portón during several field trips. They are mostly preserved as impressions in the limestones and only in few horizons the preservation is 3-D within calcareous nodules. The specimens were photographed and initial identifications were done in the field which were later corroborated by the appropriate literature in the laboratory.

### 3.3. Calcareous nannofossils

Calcareous nannofossil assemblages were recovered from 43 levels in the Pilmatué Member of the Agrio Formation at El Portón (Fig. 3). The samples were prepared following the smear slide technique of Edwards (1963). Observations and photographs were

taken using a Leica DMLP polarizing microscope with increased 1000 $\times$  magnification and accessories such as  $\lambda$  1 gypsum and blue filter. Samples were studied qualitatively considering two long transverses of the slide (range chart and a full list of all calcareous nannofossil recognized are given in the [supplementary material](#)). Calcareous nannofossils slides are stored in the Área Paleontología, Facultad de Ciencias Exactas y Naturales, Universidad de Buenos Aires, under the catalog numbers BAFC-NP 3993-4033.

## 4. Results

### 4.1. Geochronology

Eight tuff samples were collected along the Pilmatué Member of the Agrio Formation at El Portón, but only one (POT 3) was suitable for U-Pb dating. The other seven were discarded either because

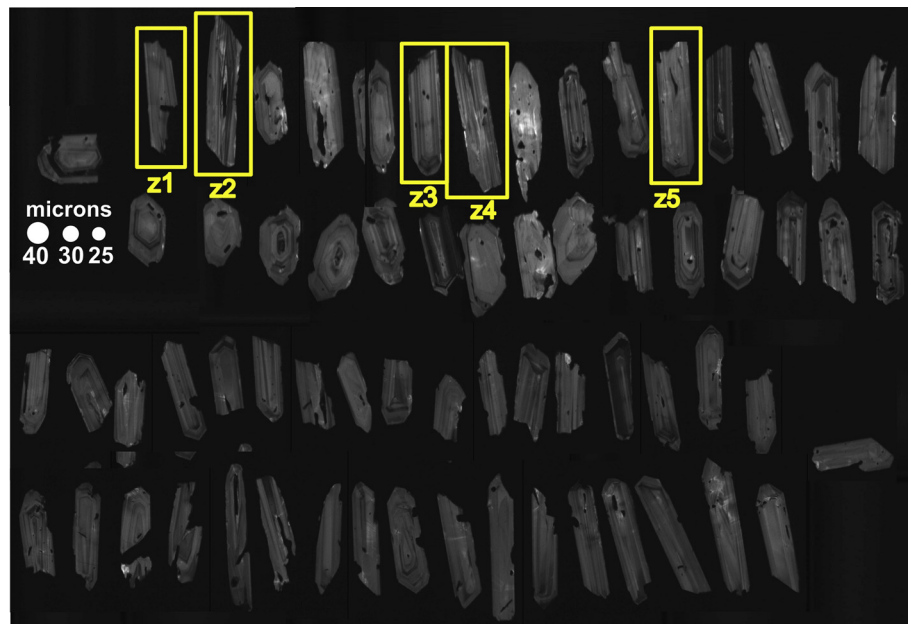


**Fig. 5.** Population of zircon crystals recovered from POT3 tuff. Grains with consistent and dominant CL patterns selected for isotopic analysis are framed and numbered, each number coinciding with data in [Table 1](#).

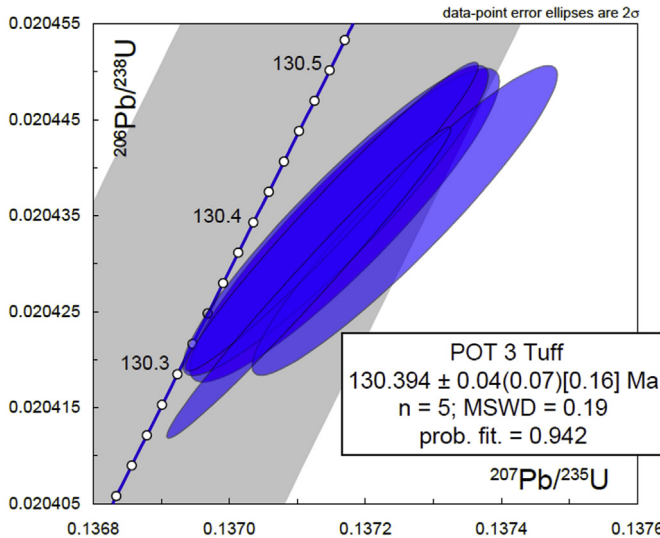


**Fig. 6.** U–Pb CA-ID-TIMS data for chemically abraded zircons from the POT 3 tuff, Pilmatué Member of the Agrio Formation (Concordia plot).

they lacked zircons or the zircons were clearly detrital. An abundant population of relatively large (approximately 100–300 micron in long dimension), elongate, prismatic zircon crystals was separated from a hand sample of POT 3 tuff.

CL-imaging of 66 high aspect ratio zircon crystals and crystal fragments from the POT 3 tuff sample revealed a consistent population of moderately to brightly luminescent, oscillatory zoned zircon. Five grains were selected for CA-TIMS analysis on the basis of CL pattern (Fig. 5). Chemical abrasion in concentrated HF at 190° for 12 h resulted in only moderate dissolution of the zircon crystals. All five analyses are concordant and equivalent, with a weighted mean  $^{206}\text{Pb}/^{238}\text{U}$  date of  $130.394 \pm 0.037(0.074)$  [0.158] Ma (MSWD = 0.19), which is interpreted as dating the eruption and deposition of this tuff (Fig. 6 and Table 1).

#### 4.2. Biostratigraphy

##### 4.2.1. Ammonites

The ammonites registered in the Pilmatué Member of the Agrio Formation at El Portón show only moderate preservation as impressions in limestones. However, based on our previous knowledge of the faunas, most of them were identified down to species level and some are illustrated in Fig. 7. Thus, the complete zonal succession of the late Valanginian–early Hauterivian ammonite faunas has been established as shown in Fig. 3.

The detailed ammonite zonal scheme in the Neuquén Basin is based on initial work by Aguirre-Urreta and Rawson (1997) with several subsequent modifications which were summarized in Aguirre-Urreta et al. (2005) and Aguirre-Urreta and Rawson (2012). During Valanginian and Hauterivian times there were 10 significant faunal turnovers in the basin (Rawson, 2007), initially reflecting an alternation of neocomitid and olcostephanid genera, then of desmoceratids and finally crioceratitid forms. As happens in NW Europe, the mid Valanginian and mid Hauterivian generalized sea-level rises are linked with the main immigration horizons which allow a correlation of the Austral Andean ammonites zones and those of the Mediterranean Province of the Tethys (Fig. 8).

The base of the *Holcoptychites neuquensis* zone lies close to the base of the Hauterivian because early *Holcoptychites* appear very close to early *Spitiidiscus* species from the lowest Hauterivian in Europe (Aguirre-Urreta and Rawson, 2003, p. 595). In addition,

**Table 1**  
U-Pb CA-ID-TIMS isotopic data of POT 3 tuff, El Portón section.

Grain <sup>a</sup>	Th/U <sup>b</sup>	$^{206}\text{Pb}^* \times 10^{-13}$ mol <sup>c</sup>	mol % $^{206}\text{Pb}$ <sup>c</sup>	Pbc (pg) <sup>c</sup>	Radiogenic isotopic ratios			Corr. coef. <sup>d</sup>	$^{207}\text{Pb}/^{235}\text{U}^e \pm \text{err}^f$	$^{206}\text{Pb}/^{238}\text{U}^e \pm \text{err}^f$
					$^{206}\text{Pb}/^{204}\text{Pb}^d$	$^{207}\text{Pb}/^{206}\text{Pb}^e$	$^{207}\text{Pb}/^{235}\text{U}^e$			
P03										
z2	0.568	1.682	99.88%	256	0.17	15146	0.181	0.048677	0.069	0.137150
z3	0.637	2.105	99.86%	221	0.25	12813	0.203	0.048680	0.078	0.137155
z4	0.570	1.519	99.85%	203	0.19	11966	0.182	0.048716	0.078	0.137258
z5	0.595	3.032	99.85%	207	0.37	12154	0.190	0.048685	0.082	0.137169
z1	0.647	2.855	99.92%	416	0.18	24050	0.207	0.048681	0.063	0.137116

<sup>a</sup> z1, z2, etc. are labels for single zircon fragments chemically abraded at 190 °C (Mattinson, 2005).

<sup>b</sup> Model Th/U ratio calculated from radiogenic  $^{208}\text{Pb}/^{235}\text{U}$  ratio and  $^{207}\text{Pb}/^{235}\text{U}$  date.

<sup>c</sup> Pb<sup>+</sup> and Pbc are radiogenic and common Pb, respectively, mol %  $^{206}\text{Pb}^*$  is with respect to total sample Pb.

<sup>d</sup> Measured ratio corrected for spike and fractionation only. Samples spiked with the ET535 tracer (Condron et al., 2015; McLean et al., 2015), with internal U fractionation correction of 0.20 ± 0.03 (1-sigma) %amu (atomic mass unit) based on analysis of ET2535-spiked samples analyzed in the same period.

<sup>e</sup> Corrected for fractionation, spike, common Pb, and initial disequilibrium in  $^{230}\text{Th}/^{238}\text{U}$ . All common Pb is assigned to procedural blank with composition of  $^{206}\text{Pb}/^{204}\text{Pb} = 18.042 \pm 0.61\%$ ;  $^{207}\text{Pb}/^{204}\text{Pb} = 15.537 \pm 0.52\%$ ;  $^{208}\text{Pb}/^{204}\text{Pb} = 37.686 \pm 0.63\%$  (1-sigma).

<sup>f</sup> Errors are 2-sigma, propagated using algorithms of Schmitz and Schoene (2007).

<sup>g</sup> Calculations based on the decay constants of Jaffey et al. (1971).  $^{206}\text{Pb}/^{238}\text{U}$  and  $^{207}\text{Pb}/^{238}\text{U}$  ratios and dates corrected for initial disequilibrium in  $^{230}\text{Th}/^{238}\text{U}$  using a mineral–melt partition coefficient ratio for  $D_{\text{Th}/\text{U}} = 0.2$ .

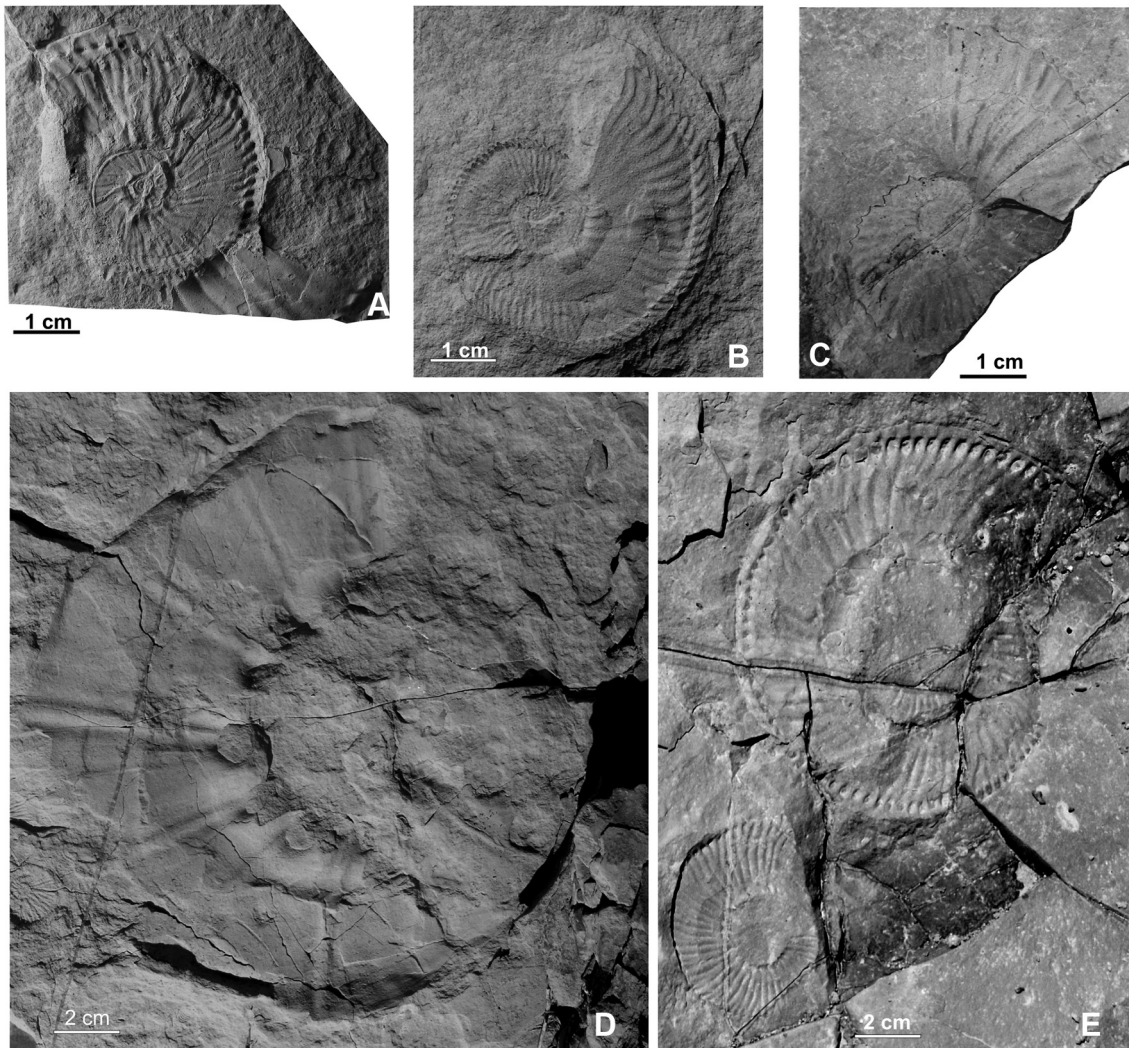


**Fig. 7.** Field photographs of representative ammonites from the El Portón section. A. *Pseudofavrella* sp. [4.5 m] B. *Decliveites agrioensis* [142 m]. C. *Holcoptychites agrioensis* [189 m]. D. *Holcoptychites magdalena* [148.5 m]. E. *Hoplitocrioceras gentilii* [228.5 m]. Numbers in square brackets indicate the stratigraphic position (meters from base of section) of each specimen.

rare *Oosterella* occur either side of the Valanginian–Hauterivian boundary in both areas (Aguirre-Urreta and Rawson, 2003, p. 607). Higher up in the faunal succession *Olcostephanus* (*Jeannoticeras*) occurs in the upper part of the *Olcostephanus* (*Olcostephanus*) *laticosta* subzone, providing a good correlation with the *Olcostephanus* (*Jeannoticeras*) *jeannoti* subzone of the *Crioceratites loryi* zone (Aguirre-Urreta and Rawson, 2001). Finally, a few specimens of *Olcostephanus* (*Olcostephanus*) *variegatus* have been recovered in the upper half of the *Hoplitocrioceras giovinei* subzone suggesting a link with the *O. (O.) variegatus* horizon of the *Lyticoceras nodosoplicatum* zone in the upper part of the lower Hauterivian (Aguirre-Urreta and Rawson, 2001).

#### 4.2.2. Calcareous nannofossils

The nannofloristic assemblage recovered from the Pilmatué Member of the Agrio Formation at El Portón, is moderately preserved, and represented by 43 species, belonging to 19 genera: *Calculites*, *Cretarhabdus*, *Cruciellipsis*, *Cyclagelosphaera*, *Diloma*, *Diazomatolithus*, *Eiffellithus*, *Helenea*, *Lithraphidites*, *Manivitella*, *Micrantholithus*, *Nannoconus*, *Percivalia*, *Retecapsa*, *Rhagodiscus*, *Staurolithites*, *Tubodiscus*, *Watznaueria* and *Zeugrhabdotus*. Some characteristic species are illustrated in Fig. 9.

Two important bioevents are recognized at El Portón. The first is the first occurrence (FO) of *Eiffellithus striatus*, which is recorded in sample BAFC-NP 3995 (Fig. 3), at a level in the middle of the *Pseudofavrella angulatiformis* ammonite subzone of Late Valanginian age. *E. striatus* occurs in numerous sections in the Neuquén Basin (Bown and Concheyro, 2004; Aguirre-Urreta et al., 2005; Concheyro et al., 2009; Lescano and Concheyro, 2009, 2014), generally first appearing at about the base of the *P. angulatiformis* zone. It is a consistent global marker, which has been found in several Mediterranean (France, Poland, Czech Republic) and Boreal (England, The Netherlands) sections and in oceanic boreholes at site 534 (Black Bahama Basin), 603 (North American margin) and 638 (Galicia margin), allowing valuable correlations (e.g. Black, 1971; Roth, 1983; Covington and Wise, 1987; Jakubowski, 1987; Bergen, 1994; Jeremiah, 2001; Morales et al., 2015). In the Tethyan Realm, Applegate and Bergen (1988) used the FO of *Eiffellithus striatus* as a marker for the base of CC4-A (Fig. 8). The CC3B and CC4A boundary has been considered Late Valanginian (Applegate and Bergen, 1988; Bergen, 1994; Gardin et al., 2000). The FO of *Eiffellithus striatus* also marks a Boreal bioevent and has been correlated with the NLK17 (Jakubowski, 1987) and BC5 (Bown, 1998) nannofossil zones of the Late Valanginian. In biostratigraphic

		AMMONITES				NANNOFOSSILS	
MEDITERRANEAN PROVINCE		NEUQUEN BASIN		MIDER. & NEUQUEN			
AGE	Zone	Sub-Zone (S) Horizon (H)	Zone	Sub-Zone	Zone	Bioevent	
L. VALANGIN. EARLY HAUTERIVIAN	<i>Lyticoceras nodosoplicatum</i>	<i>Olcostephanus (O.) variegatus H</i>	<i>Weavericeras vacaense</i>				
			<i>Hoplitocrioceras gentilii</i>	<i>Hoplitocrioceras giovinei</i>			
	<i>Crioceratites loryi</i>	<i>O. (Jeannoticeras) jeannoti S</i>			<i>Olcostephanus (O.) laticosta</i>		
		<i>Crioceratites loryi S</i>	<i>Holcoptychites neuquensis</i>		<i>Holcoptychites agrioensis</i>		CC4-A
	<i>Acanthodiscus radiatus</i>				<i>Holcoptychites neuquensis</i>		
	<i>Criosarasinella furcillata</i>	<i>Teschenites callidiscus S</i>	<i>Pseudofavrella angulatiformis</i>		<i>Decliveites crassicostatus</i>		
		<i>Criosarasinella furcillata S</i>			<i>Chacantuceras ornatum</i>		
					<i>P. angulatiformis</i>		CC3-B
							<i>E. striatus</i>
							<i>E. windii</i>

**Fig. 8.** Correlation of the late Valanginian–early Hauterivian Austral ammonite biozones in the Neuquén Basin with those of the Mediterranean Province of the Tethys (slightly modified from Reboulet et al., 2014) and the calcareous nannofossils zones and bioevents.

schemes of the North Sea Basin the FO of *Eiffellithus striatus* has been used to define the base of LK27B subzone (Jeremiah, 2001) and recently this bioevent has also been identified in North-East Greenland (Pauly et al. 2012). In recent geological time scales, the FO of *Eiffellithus striatus* has been correlated with the base of the *Criosarasinella furcillata* ammonite zone of the Mediterranean region and with Polarity Chron CM10N (Ogg and Hinnov 2012; Ogg et al., 2016). Its FO at about the base of the *angulatiformis* zone in Argentina thus supports the ammonite correlation.

*Eiffellithus windii* is another consistent marker in several Tethyan and Boreal sections and oceanic boreholes, allowing valuable correlations (e.g. Applegate and Bergen, 1988; Bergen, 1994; Bown, 1998). Its LO has been used as a bioevent for the lower Hauterivian. In the Vocomian Basin it occurs in the *Acanthodiscus radiatus* ammonite zone (Bergen, 1994) close to the Valanginian-Hauterivian boundary. However, in Boreal sections (Bown, 1998), this bioevent has been recorded higher up in the *Endemoceras regale* ammonite zone.

Particularly in El Portón section, the second nannofossil event recorded is the last occurrence (LO) of *Eiffellithus windii*, in the first sample (BAFC-NP 4017) assigned to the *Holcoptychites agrioensis* ammonite subzone, only 2.43 m above the dated tuff (Fig. 3).

The LO of *Eiffellithus windii* is considered a secondary bioevent within the CC4-A nannofossils subzone. In the Neuquén Basin, this bioevent has been identified in several sections and correlated with the *Holcoptychites neuquensis* ammonites zone (Concheyro et al., 2009; Lescano and Concheyro, 2014) and it is even higher at El Portón where it occurs at the base of the *Holcoptychites agrioensis* subzone (belonging to *Holcoptychites neuquensis* ammonites zone). This supports the correlation of the *H. agrioensis* subzone with the upper part of the *radiatus* zone of the Mediterranean region.

## 5. Discussion

In the Neuquén Basin there are up to now, four CA-ID TIMS U–Pb ages (Vennari et al., 2014; Aguirre-Urreta et al., 2015), one SHRIMP U–Pb age (Schwarz et al., 2016) and one LA-ICP-MS U–Pb age (Naipauer et al., 2015b) for the Berriasian-Hauterivian interval. There are also several LA-ICP-MS U–Pb ages for the Upper Jurassic Tordillo Formation (Naipauer et al., 2015a; Horton et al., 2016) (Fig. 10).

Vennari et al. (2014) presented a CA-ID TIMS U–Pb age of  $139.55 \pm 0.18$  Ma from a tuff interbedded with sediments carrying ammonites of early Berriasian age in the locality Las Loicas (Fig. 1A). The Tithonian–Berriasian transition is recognized in the Vaca Muerta Formation on the basis of ammonite zones and calcareous nannofossil bioevents which allow correlation with well-established Tethyan floras and faunas. Although the formal definition of the base of the Berriasian is still under consideration, those authors proposed that the J–K boundary should be close to 140 Ma.

A similar age for that boundary is implied by Naipauer et al.'s (2015b) analysis of the sedimentary environment, biostratigraphy and provenance areas of the Huncal Member of the Vaca Muerta Formation in central Neuquén (Fig. 1A). This sequence yields late Berriasian ammonites and the maximum sedimentation age, based on the youngest zircon is  $138.7 \pm 1.3$  Ma. Both dates support the proposals of Channell et al. (1995, 2010) to place the base of the Berriasian at around 141 Ma rather than the 145.7 Ma of the current timescale of Ogg et al. (2016).

Aguirre-Urreta et al. (2015) provided two precise CA-ID TIMS U–Pb ages of  $129.09 \pm 0.16$  Ma and  $127.42 \pm 0.15$  Ma from two distinct tuffs interbedded within the marine sedimentary rocks of the Agua de la Mula Member of the Agrio Formation. Both horizons

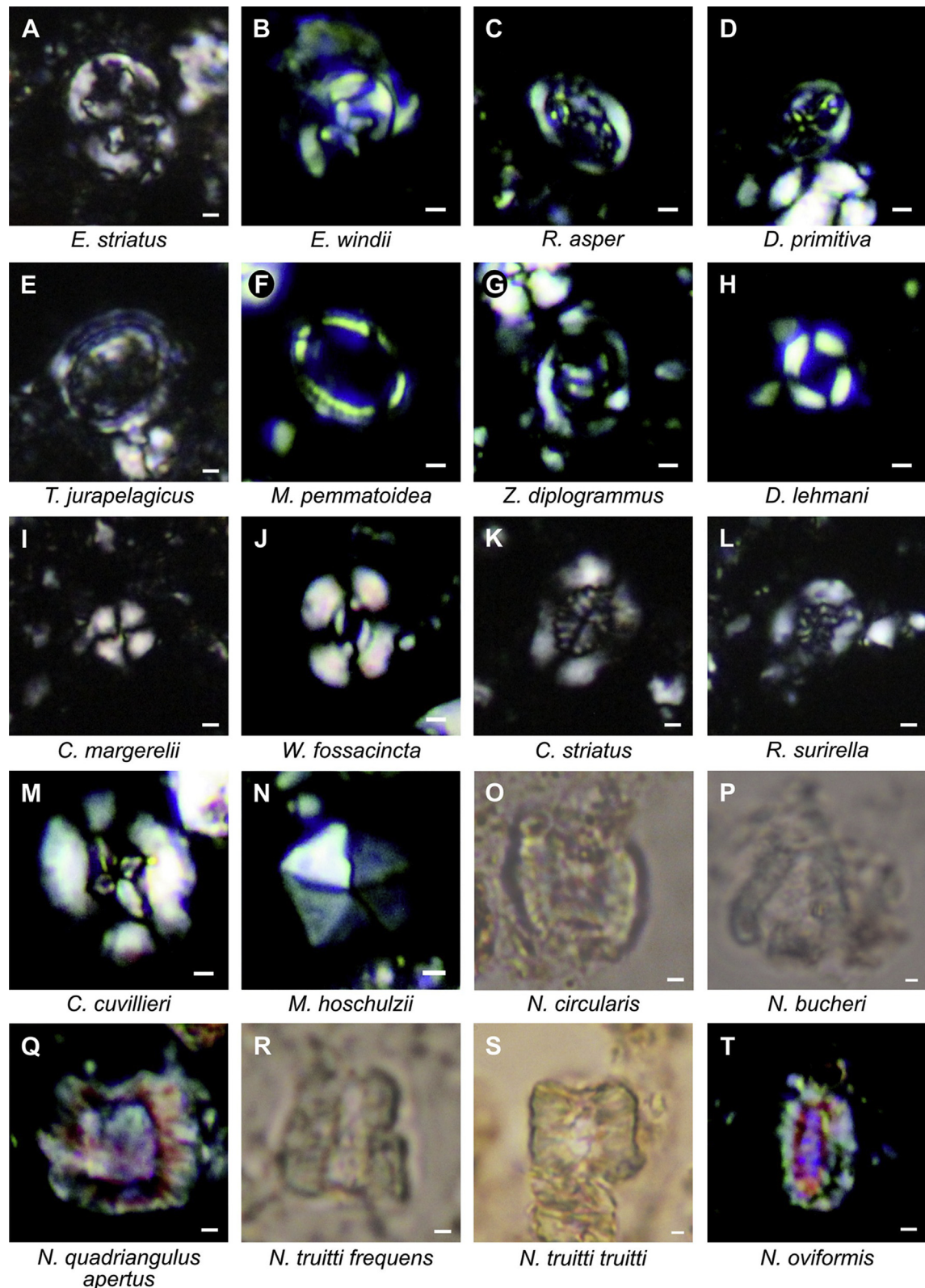
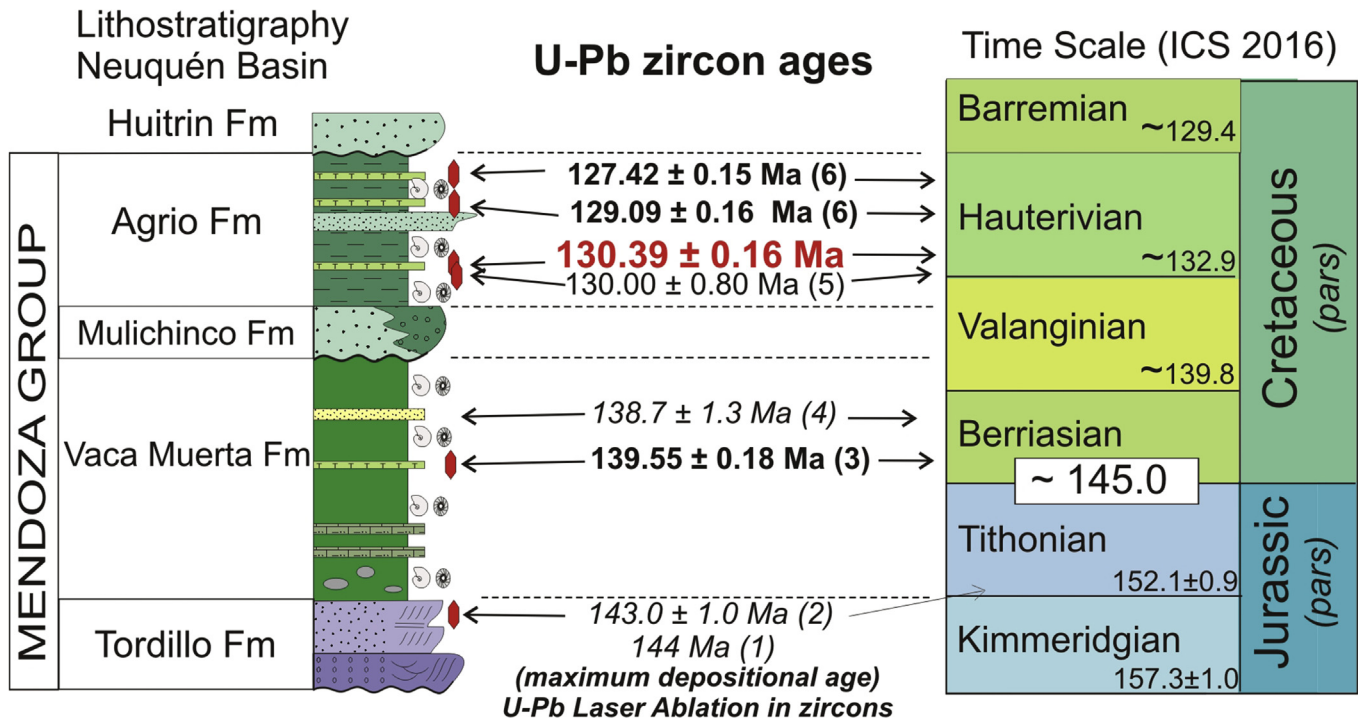


**Fig. 9.** Calcareous nannofossils from the El Portón section. Scale bar is 1  $\mu\text{m}$ . A. *Eiffellithus striatus* (Black) Applegate and Bergen (BAFC-NP 4024) [245 m]. B. *Eiffellithus windii* Applegate and Bergen (BAFC-NP 4024) [245 m]. C. *Rhagodiscus asper* (Stradner) Reinhardt (BAFC-NP 4026) [262 m]. D. *Diloma primitiva* (Worsley) Wind and Cepke (BAFC-NP 4028) [267 m]. E. *Tubodiscus jurapelagicus* (Worsley) Roth (BAFC-NP 4026) [262 m]. F. *Manivitella pemmatoidaea* (Deflandre) Thierstein (PO60, BAFC-NP 4015) [177 m]. G. *Zeugrhabdotus diplogrammus* (Deflandre) Burnett (BAFC-NP 4022) [223 m]. H. *Diazatomolithus lehmani* Nöel (PO38, BAFC-NP 4006) [130 m]. I. *Cyclagelosphaera margerellii* Nöel (BAFC-NP 4029) [279 m]. J. *Watznaueria fossacincta* (Black) Bown (BAFC-NP 3998) [50 m]. K. *Creterhabdus striatus* (Stradner) Black (BAFC-NP 4001) [77 m]. L. *Retecapsa surirella* (Deflandre and Fert) Grün (BAFC-NP 4026) [262 m]. M. *Crucielipsis cuvillieri* (Manivit) Thierstein (BAFC-NP 4000) [65 m]. N. *Micrantholithus hoschulzii* (Reinhardt) Thierstein (BAFC-NP 3998) [50 m]. O. *Nannoconus circularis* Deres and Achéritéguy (BAFC-NP 4009) [145 m]. P. *Nannoconus bucheri* Brönnimann (BAFC-NP 4028) [267 m]. Q. *Nannoconus quadriangulus apertus* Deflandre and Deflandre-Rigaud (BAFC-NP 4028) [267 m]. R. *Nannoconus trutti frequens* Deres and Achéritéguy (BAFC-NP 4028) [267 m]. S. *Nannoconus trutti trutti* Brönnimann (BAFC-NP 4029) [279 m]. T. *Nannoconus oviformis* Perch-Nielsen (BAFC-NP 4028) [267 m]. Numbers in square brackets indicate the stratigraphic position (meters from base of section) of each specimen.



- (1) Naipauer et al. 2015 a, (2) Horton et al. 2016,(3) Vennari et al. 2014  
(4) Naipauer et al. 2015 b, (5) Schwarz et al. 2016, (6) Aguirre-Urreta et al. 2015

**Fig. 10.** U–Pb zircon ages obtained in the Mendoza Group, Neuquén Basin and the discrepancies with those ages proposed as approximate numerical boundaries in the 2016 Geological Time Scale by the ICS (modified from Vennari et al., 2014). Ages in italics indicate maximum depositional ages, ages in bold indicate U–Pb CA-ID-TIMS methodology, age in normal font indicates U–Pb SHRIMP methodology.

are well constrained biostratigraphically by ammonites and calcareous nannofossils which correlate with the 'standard' sequence of the Tethyan Realm. The lower horizon (Caepe Malal locality) (Fig. 1A) is very close to the base of the upper Hauterivian, in the *Spuditiscus riccardii* ammonite biozone which correlates with the lower *Subsaynella sayni* zone of the Mediterranean Province. The upper horizon, in Agrio del Medio (Fig. 1A), is in the upper *Paraspiticeras groeberi* ammonite biozone which is correlated with the middle part of the *Pseudothurmannia ohmi* zone of the Mediterranean region (Reboulet et al., 2014), the highest Hauterivian ammonite zone. These ages indicate that the base of the upper Hauterivian lies at c. 129.5 Ma and the top at c. 127 Ma.

Schwarz et al. (2016) presented the first numerical age from the Pilmatué Member of the Agrio Formation of  $130.0 \pm 0.8$  Ma (U–Pb SHRIMP on zircons), recorded in the *Holcoptychites neuquensis* zone of early Hauterivian age in Mina San Eduardo (Fig. 1A). These authors considered that the date fitted reasonably with the latest proposed lower boundary of the Hauterivian at  $\sim 132.9$  Ma by Cohen et al. (2013). However, they did not refer to the earlier contribution of Martínez et al. (2015) who proposed a  $131.96 \pm 1.0$  Ma age for the base of the Hauterivian and a much longer duration of this period than the one recognized in the ICS time table by Cohen et al. (2013) (see below).

In the Mediterranean region of the Tethys, Martínez et al. (2015) studied the GSSP candidate for the Valanginian-Hauterivian boundary: La Charce (Vocontian Basin, SE France) and the GSSP candidate for the Hauterivian-Barremian boundary: Río Argos (Subbetic Domain, SE Spain). They anchored their astrochronology data from both sections with our U–Pb data base (Aguirre-Urreta et al., 2015) and proposed the base of the Valanginian at

$137.05 \pm 1.0$  Ma, the base of the Hauterivian at  $131.96 \pm 1.0$  Ma, and the base of the Barremian at  $126.02 \pm 1.0$  Ma. These data reinforce our differences with the current official geological time scale (International Chronostratigraphic Chart 2016/4, International Commission on Stratigraphy, ICS) and the new *A Concise Geological Time Scale 2016* (Ogg et al., 2016).

It is most unfortunate that both our high precision CA-ID TIMS U–Pb ages from the Neuquén Basin (Aguirre-Urreta et al., 2015) and Martínez et al.'s (2015) new geological time scale for the Valanginian–Hauterivian stages in the Mediterranean region integrating astrochronological and radiochronological data were not taken into consideration by Ogg et al. (2016). These authors maintain the Gradstein et al. (2012) age model for the M-sequence polarity pattern and the associated magnetostratigraphic calibrations for the Late Jurassic–Early Cretaceous interval as a working option with some slight modifications. The differences are huge, more than 2 million years for the base of the Valanginian:  $137.05 \pm 1$  Ma (Martínez et al., 2015) vs.  $139.4 \pm 0.7$  Ma (Ogg et al., 2016), nearly 3 million years for the base of the Hauterivian:  $131.96 \pm 1$  Ma (Martínez et al., 2015) vs.  $134.7 \pm 0.7$  Ma (Ogg et al., 2016), and more than 4 million years for the base of the Barremian:  $126.02 \pm 1$  Ma (Martínez et al., 2015) vs.  $130.8 \pm 0.5$  Ma (Gradstein et al., 2012; Ogg et al., 2016).

Ogg et al. (2016, p. 180) adopted those loosely-constrained ages, rather than those available to them from Argentina, until the methodological incompatibilities could be resolved "by applying magnetostratigraphy and other verifications of the chronostratigraphic ages of these important Argentina and other sections". Our correlation between the Austral Andean ammonites with those of the Mediterranean Province of the Tethys is robust, as accepted by

the Kilian Group of the ICS (Reboulet et al., 2014). The same happens with the calcareous nannofossil bioevents registered both in the Neuquén Basin and in the Mediterranean region (some of them also in the Boreal Realm) (Concheyro et al., 2009; Lescano and Concheyro, 2009, 2014; Aguirre-Urreta et al., 2015).

The present CA-ID-TIMS U–Pb ages further demonstrates the great strength and full potential of the radiometric dating of sedimentary successions by this methodology, which “is now the standard treatment for U–Pb zircon geochronology, and by dramatically reducing the degree of geological scatter in zircon data sets, it is revolutionizing the resolving power and application of ID-TIMS to geochronological problems in time scale calibration and beyond” (Schmitz, 2012, p. 117).

## 6. Concluding remarks

A high precision CA-ID TIMS U–Pb age of  $130.39 \pm 0.16$  Ma is presented here from the Pilmatué Member of the Agrio Formation in the Neuquén Basin. This absolute age is tied with ammonites and calcareous nannofossils of early Hauterivian age. This date is coherent with other two precise radioisotopic ages provided by Aguirre-Urreta et al. (2015) for the Agua de la Mula Member of the Agrio Formation of late Hauterivian age.

Martínez et al. (2015) anchored their astrochronology data from two classic sections of the Mediterranean Province, GSSP candidates for the base of the Hauterivian and the base of the Barremian, with our U–Pb data base which reinforce our differences with the 2016 ICS Geological Time Scale and that of Ogg et al. (2016). They dated the base of the Valanginian at  $137.05 \pm 1.0$  Ma, the base of the Hauterivian at  $131.96 \pm 1.0$  Ma, and the base of the Barremian at  $126.02 \pm 1.0$  Ma.

Several research projects in progress in the Neuquén Basin on magnetostratigraphy, astrochronology and more CA-ID-TIMS U–Pb zircon dating will provide further constraints to be taken into consideration in the development of a more precise Early Cretaceous Geological Time Scale.

## Acknowledgements

The authors acknowledge support from grants CONICET PIP to VAR and ANPCYT PICT 1413 to BAU, and the positive comments of two anonymous referees. This is the Contribution R-203 of the Instituto de Estudios Andinos “Don Pablo Groeber”.

## References

- Aguirre-Urreta, M.B., Rawson, P.F., 1997. The ammonite sequence in the Agrio Formation (Lower Cretaceous), Neuquén basin, Argentina. *Geological Magazine* 134, 449–458.
- Aguirre-Urreta, M.B., Rawson, P.F., 2001. Lower Cretaceous ammonites from the Neuquén Basin, Argentina: a Hauterivian *Olcostephanus* fauna. *Cretaceous Research* 22, 763–778.
- Aguirre-Urreta, M.B., Rawson, P.F., 2003. Lower Cretaceous ammonites from the Neuquén Basin, Argentina: the Hauterivian genus Holcoptychites. *Cretaceous Research* 24, 589–613.
- Aguirre-Urreta, M.B., Rawson, P.F., 2012. Lower Cretaceous ammonites from the Neuquén Basin, Argentina: a new heteromorph fauna from the uppermost Agrio Formation. *Cretaceous Research* 35, 208–216.
- Aguirre-Urreta, M.B., Rawson, P.F., Concheyro, G.A., Bown, P.R., Ottone, E.G., 2005. Lower Cretaceous (Berriasian-Aptian) biostratigraphy of the Neuquén Basin. In: Veiga, G., Spalletti, L., Howell, J.A., Schwarz, E. (Eds.), *The Neuquén Basin: a Case Study in Sequence Stratigraphy and Basin Dynamics*, Geological Society of London, Special Publication, 252, pp. 57–81.
- Aguirre-Urreta, M.B., Casadío, S., Cichowolski, M., Lazo, D.G., Rodríguez, D., 2008. Afinidades paleobiogeográficas de los invertebrados cretácicos de la cuenca Neuquina. *Ameghiniana* 45 (3), 593–613.
- Aguirre-Urreta, B., Lescano, M., Schmitz, M.D., Tunik, M., Concheyro, A., Rawson, P.F., Ramos, V.A., 2015. Filling the gap: new precise Early Cretaceous radioisotopic ages from the Andes. *Geological Magazine* 152 (3), 557–564.
- Allen, C.M., Campbell, I.H., 2012. Identification and elimination of a matrix-induced systematic error in LA-ICP-MS  $^{206}\text{Pb}/^{238}\text{U}$  dating of zircon. *Chemical Geology* 332–333, 157–165. <http://dx.doi.org/10.1016/j.chemgeo.2012.09.038>.
- Applegate, J., Bergen, J., 1988. Cretaceous calcareous nannofossil biostratigraphy of sediments recovered from the Galicia Margin, ODP Leg 103. In: Boillot, G., Winterer, E.L., Meyer, A.W., et al. (Eds.), *Proceedings of the Ocean Drilling Project, Scientific Results*, 103, pp. 293–348. College Station, Texas.
- Bergen, J., 1994. Berriasian to Early Aptian calcareous nannofossils from the Vocontian Trough (SE France) and Deep Sea Drilling Site 534: new nannofossil taxa and a summary of low-latitude biostratigraphic events. *Journal of Nannoplankton Research* 16, 59–69.
- Black, M., 1971. Coccoliths of the Speeton Clay and Sutterby Marl. *Proceedings of the Yorkshire Geological Society* 38, 381–424.
- Bown, P.R., 1998. *Calcareous Nannofossil Biostratigraphy*. British Micropaleontological Society Publication Series. Chapman and Hall, Kluwer Academic Publishers, Londres, 314 pp.
- Bown, P.R., Concheyro, A., 2004. Lower Cretaceous calcareous nannoplankton from the Neuquén Basin, Argentina. *Marine Micropaleontology* 52, 51–84.
- Channell, J.E.T., Erba, E., Nakanishi, M., Tamaki, K., 1995. Late Jurassic–Early Cretaceous timescales and oceanic magnetic anomaly block models. In: Berggren, W.A., Kent, D.V., Aubry, M., Hardenbol, J. (Eds.), *Geochronology, Time Scales and Stratigraphic Correlation*. SEPM Special Publication, 54, pp. 51–63.
- Channell, J.E.T., Casellato, C.E., Muttoni, G., Erba, E., 2010. Magnetostratigraphy, nannofossil stratigraphy and apparent polar wander for Adria-Africa in the Jurasic-Cretaceous boundary interval. *Palaeeogeography, Palaeoclimatology, Palaecology* 293, 51–75.
- Cohen, K.M., Finney, S.C., Gibbard, P.L., Fan, J.-X., 2013. The ICS International Chronostratigraphic Chart.  *Episodes* 36, 199–204.
- Concheyro, A., Lescano, M., Caramés, A., Ballent, S., 2009.  *Micropaleontología de la Formación Agrio (Cretácico inferior) en distintos sectores de la cuenca Neuquina*. Revista de la Asociación Geológica Argentina 65, 342–361.
- Condon, D.J., Schoene, B., McLean, N.M., Bowring, S.A., Parrish, R.R., 2015. Metrology and traceability of U-Pb isotope dilution geochronology (EARTHTIME Tracer Calibration Part I). *Geochimica et Cosmochimica Acta* 164, 464–480. <http://dx.doi.org/10.1016/j.gca.2015.05.026>.
- Covington, J., Wise, S., 1987. Calcareous nannofossil biostratigraphy of a Lower Cretaceous deep-sea fan complex: Deep Sea Drilling Project Leg 93 Site 603, lower continental rise off Cape Hatteras. *Initial Reports of the Deep Sea Drilling Project* 93, 617–660.
- Davydov, V.I., Crowley, J.L., Schmitz, M.D., Poletaev, V.I., 2010. High-precision U-Pb zircon age calibration of the global Carboniferous time scale and Milankovitch-band cyclicity in the Donets Basin, eastern Ukraine. *Geochemistry, Geophysics, Geosystems*. <http://dx.doi.org/10.1029/2009GC002736>.
- Edwards, A., 1963. A preparation technique for calcareous nannoplankton. *Micro-paleontology* 9, 103–104.
- Gardin, S., Bulot, L.G., Coccioni, R., De Wever, P., Hishida, K., Lambert, E., 2000. The Valanginian to Hauterivian hemipelagic successions of the Vocontian Basin (SE France): new high resolution integrated biostratigraphical data. *6th International Cretaceous Symposium* (Vienna), Abstracts: 34.
- Gradstein, F.M., Ogg, J.G., Smith, A.G., 2004. *A Geologic Time Scale 2004*. Cambridge University Press, Cambridge, 589 pp.
- Gradstein, F.M., Ogg, J.G., Schmitz, M.D., Ogg, G.M., 2012. *The Geologic Time Scale 2012*. Elsevier, Amsterdam, 1144 pp.
- Groeber, P., 1953. Ándico. In: *Geografía de la República Argentina*. Sociedad Argentina Estudios Geográficos GAEA 2(1), pp. 349–541.
- Gulisano, C.A., Gutiérrez Pleimling, A., 1988. Depósitos eólicos del Miembro Avilé (Formación Agrio, Cretácico inferior) en el norte del Neuquén, Argentina. *Segunda Reunión Argentina de Sedimentología*, Actas 120–124.
- Horton, B.K., Fuentes, F., Boll, A., Starck, D., Ramirez, S.G., Stockli, D.F., 2016. Andean stratigraphic record of the transition from backarc extension to orogenic shortening: a case study from the northern Neuquén Basin, Argentina. *Journal of South American Earth Sciences* 71, 17–40.
- Jaffey, A.H., Flynn, K.F., Glendenin, L.E., Bentley, W.C., Essling, A.M., 1971. Precision measurements of half-lives and specific activities of  $^{235}\text{U}$  and  $^{238}\text{U}$ . *Physical Review C* 4, 1889–1906.
- Jakubowski, M., 1987. A proposed Lower Cretaceous calcareous nannofossil zonation scheme for the Moray Firth area of the North Sea. *Abhandlungen der Geologischen Bundesanstalt (Wien)* 39, 99–119.
- Jeremiah, J., 2001. A Lower Cretaceous nannofossil zonation for the North Sea Basin. *Journal of Micropalaeontology* 20, 45–80.
- Lazo, D.G., Damborenea, S.E., 2011. Barremian bivalves from the Huixtán Formation, west-central Argentina: taxonomy and paleoecology of a restricted marine association. *Journal of Paleontology* 85, 719–743.
- Leanza, H.A., Hugo, C., 2001. Hoja Geológica Zapala, Hoja 3969-I, 1:250.000. Instituto de Geología y Recursos Minerales, Boletín 275, pp. 1–128.
- Legarreta, L., Uliana, M.A., 1991. Jurassic-Cretaceous marine oscillations and geometry of back-arc basin fill, central Argentine Andes. *Special Publications, International Association of Sedimentology* 12, 429–450.
- Lescano, M., Concheyro, A., 2009. Nanofósiles calcáreos de la Formación Agrio (Cretácico inferior) en el sector sudoccidental de la Cuenca Neuquina, Argentina. *Ameghiniana* 46, 73–94.
- Lescano, M., Concheyro, A., 2014. Nanocónidos del Grupo Mendoza (Cretácico Inferior) en la Provincia del Neuquén, República Argentina: Taxonomía, cronoestratigrafía e implicancias paleogeográficas. *Ameghiniana* 51, 466–499.

- Martínez, M., Deconinck, J.-F., Pellenard, P., Riquier, L., Company, M., Reboulet, S., Moiroud, M., 2015. Astrochronology of the Valanginian–Hauterivian stages (Early Cretaceous): chronological relationships between the Paraná–Etendeka large igneous province and the Weissert and the Faraoni events. *Global and Planetary Change* 131, 158–173.
- Mattinson, J.M., 2005. Zircon U-Pb chemical abrasion ("CA-TIMS") method: combined annealing and multi-step partial dissolution analysis for improved precision and accuracy of zircon ages. *Chemical Geology* 220, 47–66.
- McLean, N.M., Condon, D.J., Schoene, B., Bowring, S.A., 2015. Evaluating uncertainties in the calibration of isotopic reference materials and multi-element isotopic tracers (EARTHTIME Tracer Calibration Part II). *Geochimica et Cosmochimica Acta* 164, 481–501. <http://dx.doi.org/10.1016/j.gca.2015.02.040>.
- Morales, C., Kujau, A., Heimhofer, U., Mutterlose, J., Spangenberg, J.E., Adatte, T., Ploch, I., Föllmi, K.B., 2015. Palaeoclimate and palaeoenvironmental changes through the onset of the Valanginian carbon–isotope excursion: evidence from the Polish Basin. *Palaeogeography, Palaeoclimatology, Palaeoecology* 426, 183–198.
- Naipauer, M., Tunik, M., Marques, J.C., Rojas Vera, E.A., Vujovich, G.I., Pimentel, M.M., Ramos, V.A., 2015a. U-Pb detrital zircon ages of Upper Jurassic continental successions: implications for the provenance and absolute age of the Jurassic–Cretaceous boundary in the Neuquén Basin. In: Sepúlveda, S., Giambiagi, L., Moreira, S., Pinto, L., Tunik, M., Hoke, G., Farías, M. (Eds.), *Geodynamic Processes in the Andes of Central Chile and Argentina*, 399. Geological Society, Special Publications, London, pp. 131–154.
- Naipauer, M., Lescano, M., Zavala, C., Aguirre-Urreta, B., Pimentel, M., Ramos, V.A., 2015b. Estudio multidisciplinario en la Formación Vaca Muerta: ambiente de sedimentación, bioestratigrafía, edades U-Pb en circones y áreas de proveniencia del Miembro Huncal. XIV Congreso Geológico Chileno (La Serena), Resúmenes Expandidos Electrónicos, 4 pp.
- Nasdala, L., Lengauer, C.L., Hanchar, J.M., Kronz, A., Wirth, R., Blanc, P., Kennedy, A.K., Seydoux-Guillaume, A.M., 2002. Annealing radiation damage and the recovery of cathodoluminescence. *Chemical Geology* 191, 121–140.
- Ogg, J.G., Hinnov, L.A., 2012. Cretaceous. In: Gradstein, F., Ogg, J.G., Schmitz, M.D., Ogg, G.M. (Eds.), *The Geologic Time Scale 2012*. Elsevier, Amsterdam, pp. 793–853.
- Ogg, J.G., Ogg, G., Gradstein, F.M., 2008. *A Concise Geologic Time Scale 2016*. Cambridge University Press, Cambridge, 177 pp.
- Ogg, J.G., Ogg, G., Gradstein, F.M., 2016. *The Concise Geologic Time Scale*. Elsevier, 234 pp.
- Pauly, S., Mutterlose, J., Alsen, P., 2012. Lower Cretaceous (upper Ryazanian–Hauterivian) chronostratigraphy of high latitudes (North-East Greenland). *Cretaceous Research* 34, 308–326.
- Ramos, V.A., 2010. The tectonic regime along the Andes: present-day and Mesozoic regimes. *Geological Journal* 45, 2–25.
- Ramos, V.A., Folguera, A., 2005. Tectonic evolution of the Andes of Neuquén: constraints derived from the magmatic arc and foreland deformation. In: Veiga, G., Spalletti, L., Howell, J.A., Schwarz, E. (Eds.), *The Neuquén Basin: a Case Study in Sequence Stratigraphy and Basin Dynamics*, 252. Geological Society of London, Special Publication, London, pp. 15–35.
- Rawson, P.F., 2007. Global relationships of Argentine (Neuquén Basin) Early Cretaceous ammonite faunas. *Geological Journal* 42, 175–183.
- Reboulet, S., Szives, O., Aguirre-Urreta, B., Barragán, R., Company, M., Idakieva, V., Ivanov, M., Kakabadze, M.V., Moreno-Bedmar, J.A., Sandoval, J., Baraboshkin, E.J., Çağlar, M.K., Fözy, I., González-Arreola, C., Kenjo, S., Lukeneder, A., Raisossadat, S.N., Rawson, P.F., Tavera, J.M., 2014. Report on the 5th International Meeting of the IUGS Lower Cretaceous Ammonite Working Group, the "Kilian Group" (Ankara, Turkey, 31st August 2013). *Cretaceous Research* 50, 126–137.
- Remane, J., 2000. International Stratigraphic Chart, with Explanatory Note. Sponsored by ICS, IUGS and UNESCO. 31st International Geological Congress, Rio de Janeiro, 16 pp.
- Roth, P., 1983. Jurassic and Lower Cretaceous Calcareous Nannofossils in the Western North Atlantic (Site 534): biostratigraphy, preservation, and some observations on biogeography and paleoceanography. *Initial Reports of the Deep Sea Drilling Project* 76, 587–621.
- Schmitz, M.D., 2012. Radiogenic Isotope Geochronology. In: Gradstein, F., Ogg, J.G., Schmitz, M.D., Ogg, G.M. (Eds.), *The Geologic Time Scale 2012*. Elsevier, Amsterdam, pp. 115–126.
- Schmitz, M.D., Davydov, V.I., 2012. Quantitative radiometric and biostratigraphic calibration of the Pennsylvanian-Early Permian (Cisuralian) time scale and pan-Euramerican chronostratigraphic correlation. *Geological Society of America Bulletin* 124, 549–577.
- Schmitz, M.D., Schoene, B., 2007. Derivation of isotope ratios, errors and error correlations for U-Pb geochronology using  $^{205}\text{Pb}$ - $^{235}\text{U}$ - $^{233}\text{U}$ -spiked isotope dilution thermal ionization mass spectrometric data. *Geochemistry, Geophysics, Geosystems* 8, Q08006. <http://dx.doi.org/10.1029/2006GC001492>.
- Schwarz, E., Spalletti, L.A., Veiga, G.D., Fanning, C.M., 2016. First U-Pb SHRIMP age for the Pilmatue Member (Agrio Formation) of the Neuquén Basin, Argentina: implications for the Hauterivian lower boundary. *Cretaceous Research* 58, 223–233.
- Veiga, G.D., Spalletti, L.A., Flint, S., 2002. Aeolian/fluvial interactions and high-resolution sequence stratigraphy of a non-marine lowstand wedge: the Avilé Member of the Agrio Formation (Lower Cretaceous), central Neuquén Basin, Argentina. *Sedimentology* 49, 1001–1019.
- Vennari, V.V., Lescano, M., Naipauer, M., Aguirre-Urreta, B., Concheyro, A., Schaltegger, U., Armstrong, R., Pimentel, M., Ramos, V.A., 2014. New constraints on the Jurassic-Cretaceous boundary in the High Andes using high-precision U-Pb data. *Gondwana Research* 26, 374–385.
- Vergani, G.D., Tankard, A.J., Belotti, H.J., Welsink, H.J., 1995. Tectonic evolution and paleogeography of the Neuquén Basin, Argentina. In: Tankard, A.J., Suárez, S.R., Welsink, H.J. (Eds.), *Petroleum Basins of South America*, AAPG Memoir 62, pp. 383–402.
- Weaver, C.E., 1931. Paleontology of the Jurassic and Cretaceous of West Central Argentina. *Memoir of the University of Washington* 1, 1–469.

## Appendix A. Supplementary data

Supplementary data related to this article can be found at <http://dx.doi.org/10.1016/j.cretres.2017.03.027>.